Tellus
SERIES B
CHEMICAL
AND PHYSICAL
METEOROLOGY
PUBLISHED BY THE INTERNATIONAL METEOROLOGICAL INSTITUTE IN STOCKHOLM

Tellus (2010), 62B, 608–620

Decadal change of dissolved inorganic carbon in the subarctic western North Pacific Ocean

By M. WAKITA[1,2]*, S. WATANABE[1], A. MURATA[2], N. TSURUSHIMA[3] and M. HONDA[2],
[1]*Mutsu Institute for Oceanography, Japan Agency for Marine-Earth Science and Technology, 690 Kitasekine, Sekine, Mutsu, Aomori 035-0022, Japan;* [2]*Research Institute for Global Change, Japan Agency for Marine-Earth Science and Technology, 2-15 Natsushima-Cho, Yokosuka, Kanagawa 237-0061, Japan;* [3]*Research Institute for Environment Management Technology, National Institute of Advanced Industrial Science and Technology, 16-1 Onogawa, Tsukuba, Ibaraki 305-8569, Japan*

(Manuscript received 30 November 2009; in final form 14 June 2010)

ABSTRACT

Dissolved inorganic carbon (DIC) was measured from 1992 to 2008 at two time-series sites in the subarctic western North Pacific; this region is a source of atmospheric CO_2 in winter due to vertical mixing of deep waters rich in DIC. To estimate the decadal DIC increase resulting from CO_2 uptake from the atmosphere, we corrected DIC for the contribution of biological activity below the temperature minimum (T_{min}) layer (∼100 m), which is the remnant of the mixed layer from the preceding winter. Decadal DIC increases in the T_{min} layer and upper intermediate water (1.3–1.5 μmol kg^{-1} yr^{-1}; 100–200 m) were higher than those expected from oceanic equilibration with increasing atmospheric CO_2 and those previously reported in the open North Pacific. The increase in water column CO_2 was estimated to be 0.40 ± 0.08 mol m^{-2} yr^{-1}. The decadal DIC change in the T_{min} layer affects winter CO_2 emission. The increase of atmospheric xCO_2 in winter (2.1 ± 0.0 ppm yr^{-1}) is higher than that of oceanic xCO_2 (0.7 ± 0.5 ppm yr^{-1}) that calculated from DIC and total alkalinity in the T_{min} layer. This difference suggests reduction of CO_2 emission in winter is possibly controlled by the increase of total alkalinity.

1. Introduction

Anthropogenic CO_2 was taken up by the global ocean at a rate of 2.2 ± 0.4 PgC yr^{-1} during the 1990s (Denman et al., 2007). The most fundamental and reliable approach to the direct detection of the CO_2 uptake rate and its variation is to make more accurate and longer time-series observations at fixed stations, for example, station ALOHA in the subtropical North Pacific Ocean (e.g. Dore et al., 2003), BATS in the subtropical western North Atlantic Ocean (e.g. Bates et al., 2002), ESTOC in the subtropical eastern North Atlantic Ocean (e.g. Santana-Casiano et al., 2007), Ocean Station Papa (OSP) in the subarctic eastern North Pacific (e.g. Wong and Chan, 1991) and stations KNOT (44°N, 155°E) (e.g. Tsurushima et al., 2002) and K2 (47°N, 160°E) (e.g. Honda et al., 2006) in the subarctic western North Pacific Ocean (Fig. 1). Time-series observations are essential to understanding temporal variation of dissolved inorganic carbon (DIC) in the ocean.

Increases of DIC in the surface waters from 1997 to 2001 and in the subsurface waters from 1992 to 2001 were detected by time-series observations at KNOT (Tanaka et al., 2003; Wakita et al., 2005). DIC is positively correlated with AOU in the subsurface water due to the decomposition of organic matter. AOU was calculated by subtracting the observed concentration of dissolved oxygen (DO) from the saturated concentration calculated from temperature and salinity with the equation of Weiss (1970). A linear increase in AOU is superimposed on a bidecadal oscillation of AOU in the Oyashio region (near the subarctic western North Pacific) (Ono et al., 2001). Because the previously reported DIC increases in the subarctic western North Pacific are based on time-series data only from the 10-year period 1992 to 2001 (Wakita et al., 2005), more accurate and longer time-series data are required to confirm the increase of DIC.

At least annually since 1997, the Japan Agency for Marine-Earth Science and Technology (JAMSTEC) has conducted hydrographic observations at KNOT or K2 in the subarctic western North Pacific (Fig. 1). Hydrographic studies in this region were also conducted by other organizations between 1992 and 2003 (e.g. Tsurushima et al., 2002; Wakita et al., 2005). In this study,

*Corresponding author.
e-mail: mwakita@jamstec.go.jp
DOI: 10.1111/j.1600-0889.2010.00476.x

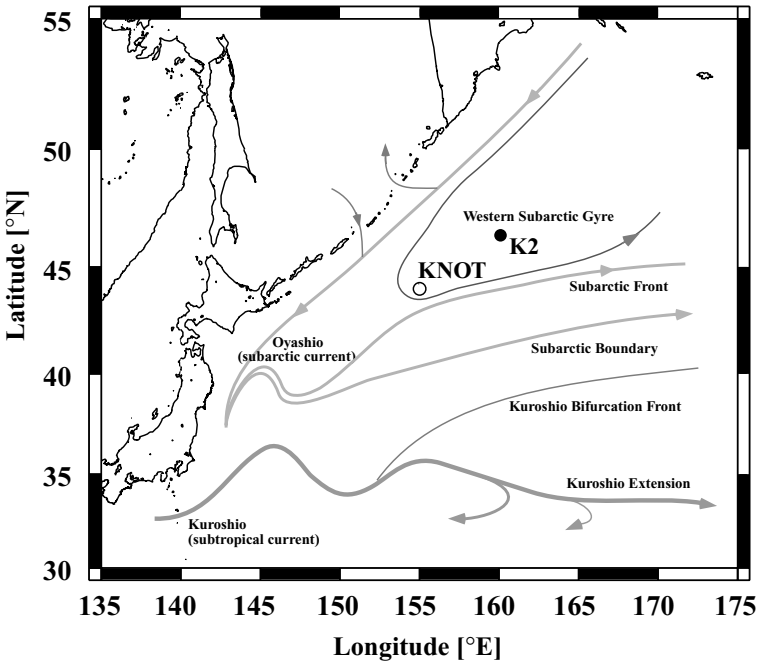

Fig. 1. Sampling stations and main ocean currents in the subarctic western North Pacific. The Kuroshio and Oyashio are the subtropical and subarctic western boundary currents in this region, respectively. This is modified from Yasuda et al. (1996).

we compiled data obtained by JAMSTEC and others and investigated the temporal variation of DIC and related properties [AOU and total alkalinity (TA)] below the winter mixed layer of the subarctic western North Pacific for 1992–2008. We also discuss the decadal increase of DIC resulting from the uptake of CO_2 from the atmosphere through gas exchange at the air–sea interface.

2. Data sources and analyses

We prepared a set of data to investigate long-term climate change in the subarctic western North Pacific. All data were collected from the observations at the Japanese time-series stations KNOT and K2 from 1992 to 2008, which were made in 61 CTD casts on 44 cruises at KNOT and in 28 CTD casts on 15 cruises at K2; these cruises were made by seven research vessels: T/S *Hokusei Maru* (Hokkaido University), T/S *Oshoro Maru* (Hokkaido University), R/V *Bosei Maru* (Tokai University), R/V *Hakuho Maru* (Tokyo University), R/V *Kaiyo Maru* (Japan Fisheries Agency), R/V *Hakurei No. 2* (Metal Mining Agency of Japan), R/V *Natsushima* (JAMSTEC) and R/V *Mirai* (JAMSTEC) (Tsurushima et al., 2002; Wakita et al., 2005; Watanabe et al., 2007). Approximately, 60% of all observations were done from the R/V *Mirai*. Data sets from K2 from 1999 to 2006 (Watanabe et al., 2007) are published at the Carbon Dioxide Information and Analysis Center (http://cdiac.ornl.gov/) and the JAMSTEC data web site (http://www.godac.jamstec.go.jp/k2/index.html). DIC and TA were measured by using coulometric and potentiometric techniques, respectively. The precision of both DIC and TA was ±0.1% or better from duplicate determinations. TA from July 2000 to July 2001 during T/S *Hokusei Maru* cruise was determined by the improved single-point titration method, with precision of ±0.2% from duplicate determinations (Wakita et al., 2005). The DIC and TA values were determined with calibration against certified reference material provided by Prof. A. G. Dickson (Scripps Institution of Oceanography). The DO and nutrient concentrations from JAMSTEC observations were measured with an automatic titrator and a continuous flow analyser, respectively (e.g. Watanabe et al., 2007). We merged the KNOT data obtained by JAMSTEC cruises with those published by Wakita et al. (2005) and Tsurushima et al. (2002) for T/S *Hokusei Maru*, T/S *Oshoro Maru*, R/V *Bosei Maru* and R/V *Hakuho Maru* cruises. In addition, we added the oceanic physical and chemical data from KNOT and K2 collected as part of WOCE–P1 (1999) (http://whpo.ucsd.edu/data_access/show_cruise?ExpoCode=49KA199905_1) and WESTCOSMIC (1998, 1999) (http://www.kanso.co.jp/ocean/html-doc/english/top1.html).

The values of DIC, TA, DO and nutrients (silicate, phosphate and nitrate) had systematic errors among cruises, because the analytical methods used for these determinations and the precision and standards for analysis varied slightly from cruise to cruise. These systematic errors probably derive from the standardization because of the absence of a common reference material. DIC data for 1992–1997 during T/S *Hokusei Maru* cruise by Wakita et al. (2005) were not calibrated against certified reference material.

To investigate the temporal variation of chemical properties from the winter mixed layer to intermediate water, we corrected the systematic errors by assuming that ocean chemical

properties in the North Pacific Deep Water (NPDW) were constant in our study area from 1992 to 2008 (Wakita et al., 2005; Watanabe et al., 2007). NPDW was defined as the water mass between 27.69σ_θ (~2000 db) and 27.77σ_θ (~3500 db), because chlorofluorocarbons were not detected below 27.69σ_θ (Watanabe et al., 2001) and the bottom water deeper than the NPDW in the western North Pacific expanding from the Samoan Passage is characterized by potential temperature (θ) lower than 1.2 °C (≈27.77σ_θ) (Johnson et al., 1994). Because the residence time of NPDW is ~500 years (Stuiver et al., 1983), we can assume that the NPDW did not change significantly from 1992 to 2008 for the purpose of investigating the temporal variations in shallower waters.

The values of the systematic errors and factors were –6–19 μmol kg^{-1} for DIC, –15–8 μmol kg^{-1} for TA, 0.82–0.97 for DO, 0.95–1.09 for silicate, 0.98–1.12 for phosphate and 0.96–1.04 for nitrate. We corrected the values of these properties at the isopycnal surfaces of NPDW (σ_θ = 27.69, 27.70, 27.71, 27.72, 27.73, 27.74, 27.75, 27.76 and 27.77) to fit the mean observed values from 2006 to 2008 at the same isopycnal surfaces. The values at each of these isopycnal surfaces were obtained by linear interpolation. The minimum systematic errors were ±0.2% for DIC and TA, ±3% for DO and ±1% for nutrients. The standard deviations of DIC, TA, DO, silicate, phosphate and nitrate values in NPDW after the corrections were estimated to be ±1.9, ±1.3, ±1.5, ±1.0, ±0.01 and ±0.1 μmol kg^{-1}, respectively. These values agree well with the measurement precision for these properties and serve for use in evaluations of the temporal variation of chemical properties.

Because KNOT and K2 are both located in the western subarctic gyre (Fig. 1) and we lacked sufficient decadal time-series data for either station, we combined data from KNOT and K2. The typical water column structure in this region has a minimum temperature ($T_{\min}$) layer at about 26.5σ_θ (~100 m), which is the remnant of the mixed layer from the preceding winter; the maximum temperature layer is at about 27.1σ_θ (~370 m) (Fig. 2) (e.g. Osafune and Yasuda, 2006). Because KNOT is located just North of the Subarctic Front (Fig. 1), data obtained there on some days (10 and 11 May 1999 (MR99–K02); 5 June 1999 (HO99–1); 22 July 1999 (HO99–3)) include no $T_{\min}$ layer as a result of the migration of subtropical water (Tsurushima et al., 2002). Data from these days were excluded from the analysis of the $T_{\min}$ layer in this study.

We here define the $T_{\min}$ layer as the remnant of the winter mixed layer in early April, when the surface mixed layer was the coldest in the year (Fig. 3a). The depth, salinity and σ_θ of the surface mixed layer reached annual maxima from middle March to early April (Figs 3b–d). Because the mean values of depth and σ_θ in the winter mixed layer in early April (~120 m, ~26.5 kg m^{-3}) were similar to those of the $T_{\min}$ layer over all season from 1992 to 2008 (108 ± 18 m, 26.5 ± 0.1 kg m^{-3}) (Figs 3b and c), in the $T_{\min}$ layer there was no influence of the surface mixed layer from spring to fall. We can thus define the $T_{\min}$ layer as the remnant of the winter mixed layer in early April.

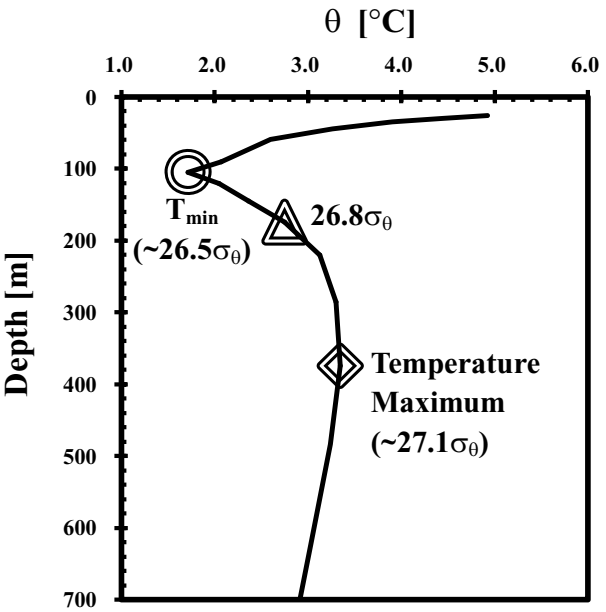

Fig. 2. Typical vertical profile of potential temperature (θ) in the western subarctic gyre by using averages of all data from 1992 to 2008 at stations KNOT and K2. The symbols show the temperature minimum ($T_{\min}$) layer (circles) and temperature maximum layer (diamonds).

The values of properties on each isopycnal surface (26.6σ_θ–27.1σ_θ) were obtained by linear interpolation of discrete bottle sampling data. For the $T_{\min}$ layer, after the values of $T_{\min}$, depth, salinity and σ_θ were determined from continuous CTD data (1 db resolution), the contents of chemical parameters (DO, DIC, TA and nutrients) on the $T_{\min}$ isopycnal surface were obtained by linear interpolation of discrete bottle sampling data. This was done because the values of depth, salinity and σ_θ in the $T_{\min}$ layer are not necessarily identical to those from discrete bottle sampling.

3. Results and discussion

3.1. Seasonal variations of DIC and related properties in the surface water

In winter, the western subarctic gyre is a source of atmospheric CO_2 because of strong vertical mixing; from spring to fall it is a sink for CO_2 because of biological production (e.g. Tsurushima et al., 2002; Kawakami et al., 2007). At KNOT and K2, the maximum values of pCO_2 and net air–sea CO_2 flux occurred in early April (late winter); these maximum values were larger than the climatological mean values for this region reported by Takahashi et al., 2009 (Figs 3i and j). The values of pCO_2 in the ocean were calculated from DIC and TA by using the CO2SYS program (Pierrot et al., 2006), by using all data

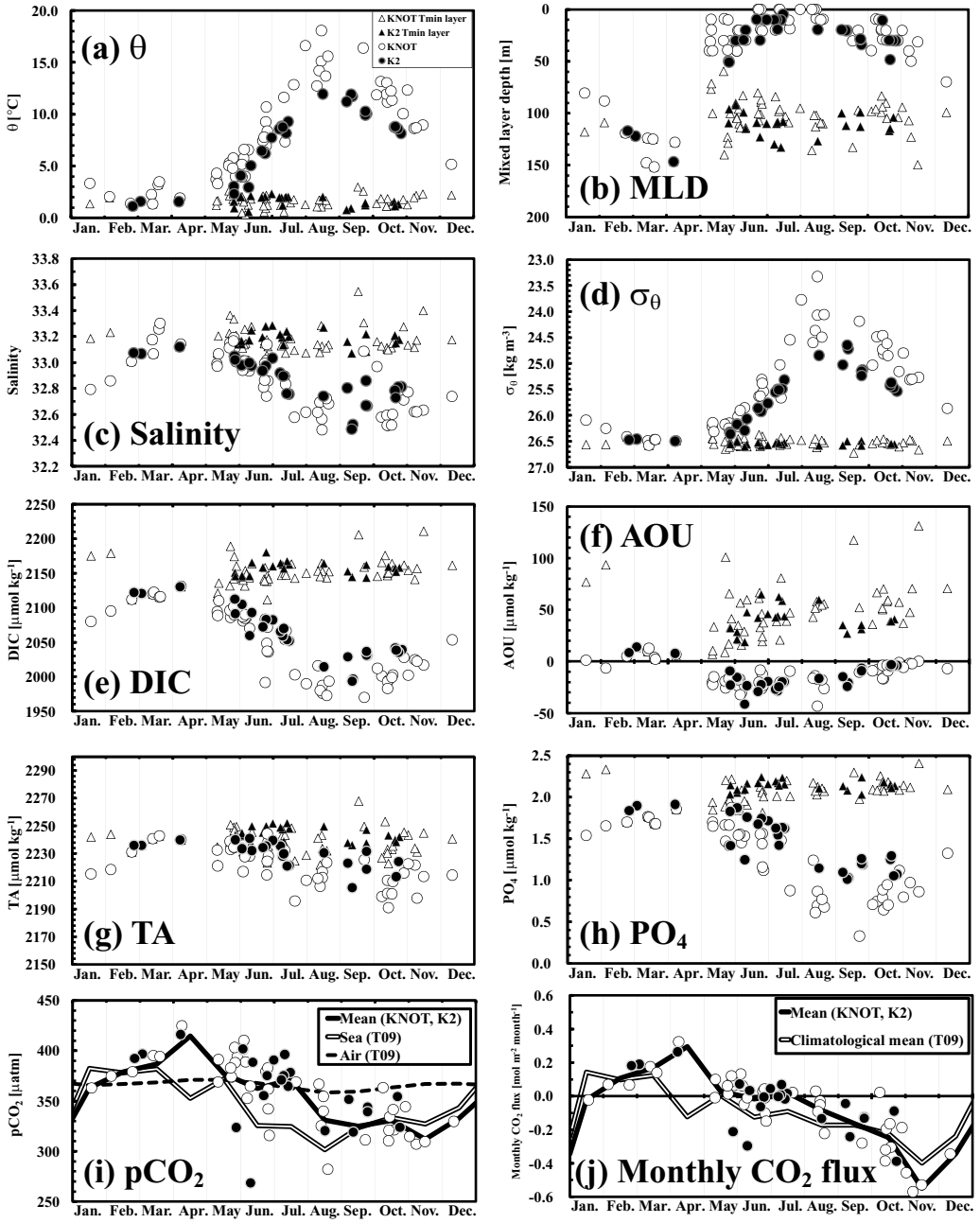

Fig. 3. Seasonal variations of (a) θ, (b) maximum mixed layer depth (MLD), (c) salinity, (d) σ_θ, (e) DIC, (f) AOU, (g) TA and (h) phosphate (PO_4) in the surface mixed layer (circles) and minimum temperature (T_{min}) layer (triangles) at stations KNOT (open symbols) and K2 (solid symbols). We also show the seasonal variations of (i) oceanic and atmospheric pCO_2 and (j) monthly net air–sea CO_2 flux in the surface mixed layer. These figures were plotted by using all data from 1992 to 2008 in order to examine the typical features of seasonal variations at KNOT and K2 and to compare them with the climatological monthly mean from Takahashi et al. (2009). The density criterion in the surface mixed layer was smaller than 0.125 kg m^{-3} (de Boyer Montégut et al., 2004). Values of oceanic pCO_2 (i) were calculated from TA and DIC. The individual pCO_2 values calculated in different years are normalized to a reference year 2000 using 1.5 μatm $year^{-1}$ as the rate of pCO_2 increase (Takahashi et al., 2009). Values of monthly net air–sea CO_2 flux (j) were estimated with the sea–air pCO_2 difference at KNOT and K2 and the climatological monthly mean value of air–sea gas transfer rate for 48°N, 157.5°E as the center of a 4° (latitude) × 5° (longitude) grid cell that is parameterized as a function of (wind speed)^2 with a scaling factor of 0.26 from Takahashi et al. (2009) (T09). Positive values indicate effluxes from the sea and negative values influxes from the air. The thick black lines in (i) and (j) are the monthly mean values averaged for KNOT and K2. The other lines in (i) are pCO_2 in the seawater (doublet) and in the atmosphere (thin dash) and the doublet line in (j) is the monthly net air–sea CO_2 flux. These values are the climatological monthly mean values at 48°N, 157.5°E, the center of the designated box from Takahashi et al. (2009).

from 1992 to 2008 to examine the typical features of seasonal variation. In this calculation, we used the carbonate dissociation constants of Mehrbach et al. (1973) as refitted by Dickson and Millero (1987). The other properties also reached annual maxima in late winter (Fig. 3): mixed layer depth (∼135 m), salinity (∼33.2), σ_θ (∼26.5 kg m^{-3}), DIC (∼2130 μmol kg^{-1}), AOU (∼8 μmol kg^{-1}), TA (∼2 240 μmol kg^{-1}) and phosphate (∼1.9 μmol kg^{-1}). The amplitude of seasonal variation of DIC in the surface mixed layer at KNOT (∼160 μmol kg^{-1}) was larger than that at K2 (∼130 μmol kg^{-1}) (Fig. 3e). These amplitudes in the western subarctic gyre are larger than those at other pelagic ocean time-series sites and are mainly attributed to biological production from spring to fall and strong vertical mixing in winter (e.g. Tsurushima et al., 2002). In summer, DIC and phosphate were lower at KNOT than at K2 (Figs 3e and h), which suggests that the difference of seasonal amplitude between KNOT and K2 is caused by differences in biological production (Kawakami et al., 2007). The values of DIC, AOU, TA, phosphate, pCO_2 and net air–sea CO_2 flux in winter (early April) at KNOT were similar to those in winter at K2 (Fig. 3). During winter, there were no differences in biological production and CO_2 emission between KNOT and K2. CO_2 emission during winter is controlled by strong vertical mixing of subsurface waters rich in DIC, TA and nutrients because of decomposition of organic matter and dissolution of $CaCO_3$ (e.g. Takahashi et al., 2006). These results indicate that the decadal DIC increase in the T_{min} layer is affected by not only the increase of anthropogenic CO_2, but also the temporal variation of CO_2 emission in winter due to strong vertical mixing.

3.2. *Temporal variations of DIC and related properties in the subsurface water*

We detected distinct trends in θ, salinity and isopycnal depths in the T_{min} and 26.6–26.8σ_θ layers (Fig. 4, Table 1). There was no apparent DIC increase observed in the subsurface water and AOU significantly decreased in the 26.6–26.8σ_θ layer ($P < 0.05$) (Fig. 5, Table 1), even though DIC and AOU reportedly increased from 1992 to 2001 at KNOT (Wakita et al., 2005). These linear regressions model was fitted using the least squares approach.

Long-term trends and bidecadal oscillations of values of θ, salinity, isopycnal depth, AOU and nutrients in the subsurface water in the northwestern subarctic Pacific Ocean are known (Ono et al., 2001; Osafune and Yasuda, 2006; Watanabe et al., 2008). Recently, the bidecadal oscillations were linked to the nodal tidal cycle with an 18.6-year period (e.g. Osafune and Yasuda, 2006), in addition to the already known linkage to the bidecadal component of North Pacific Index (NPI) (Trenberth and Hurrell, 1994; Ono et al., 2001). The isopycnal depths, θ, salinity and AOU in the intermediate water are decreasing when the diurnal tide is strengthening, which occurred from the late 1990s to the late 2000s. It has also been reported that T_{min} in the Oyashio upstream (near the subarctic western North Pacific) has a tendency to warm in the periods when the diurnal tide is both strong in the late 1990s and weak in the late 2000s (Osafune and Yasuda, 2006).

Decadal variations of DIC and AOU should be affected by this oscillation. However, we did not detect such DIC and AOU variations in our data collected during 1992–2008, because this period is shorter than a bidecadal cycle and because diurnal tide strengthening occurred from the late 1990s to the late 2000s (e.g. Osafune and Yasuda, 2006). A declining tendency of AOU was observed from the late 1990s (Fig. 5a), which is consistent with the AOU decrease observed from 1997 to 2006 in the North Pacific (Mecking et al., 2008). Because DIC is positively correlated with AOU in the subsurface water ($r = 0.99$) due to the decomposition of organic matter, decadal trends of DIC corrected for the contribution of organic matter decomposition should be detectable and larger than the decadal DIC trend we observed from 1992 to 2008.

TA significantly increased at rates of 0.5–1.6 μmol kg^{-1} yr^{-1} in the subsurface water ($P < 0.05$) (Fig. 5c, Table 1), despite the lack of a linear trend in TA at KNOT from 1997 to 2001 (Wakita et al., 2005). Also, the increase of potential alkalinity (PA), which is defined as the sum of TA and nitrate and is used to estimate the change in the dissolution of $CaCO_3$, was in the range of 0.5–1.7 μmol kg^{-1} yr^{-1} (not shown). The saturation depths of aragonite and calcite were calculated at about 120 m (∼26.6σ_θ) and 170 m (∼26.8σ_θ) from TA and DIC data and the CO2SYS program (Pierrot et al., 2006), respectively. Those depths are consistent with previously published results (Feely et al., 2002). The observed TA and PA trends might have been caused by the increase of $CaCO_3$ dissolution resulting from the DIC increase, because anthropogenic CO_2 accumulates below the saturation depth of aragonite (∼120 m) in the western subarctic gyre; this saturation depth is shallower than that in the open North Pacific (Feely et al., 2002). This trend is comparable to the TA increases between GEOSECS (early 1970s) and WOCE (early 1990s) estimated by Sarma et al. (2002), which was 0.6 ± 0.4 μmol kg^{-1} yr^{-1} in the aragonite saturation horizons of the subarctic region in the North Pacific.

3.3. *Estimate of DIC increase due to air–sea CO_2 gas exchange*

The change in DIC in the subsurface water is controlled by the uptake of atmospheric CO_2 through gas exchange at the air–sea interface, the decomposition of organic matter and the dissolution of $CaCO_3$ (e.g. Gruber et al., 1996; Sabine et al., 2002). The decomposition of organic matter includes oxidation and denitrification of organic matter in the subsurface seawater (e.g. Sabine et al., 2002). Oxidation and denitrification of organic matter are related to AOU and N^* [=(nitrate + nitrite) − 16 × (phosphate) + 2.90] as an index of nitrogen fixation–denitrification (Deutsch et al., 2001), respectively.

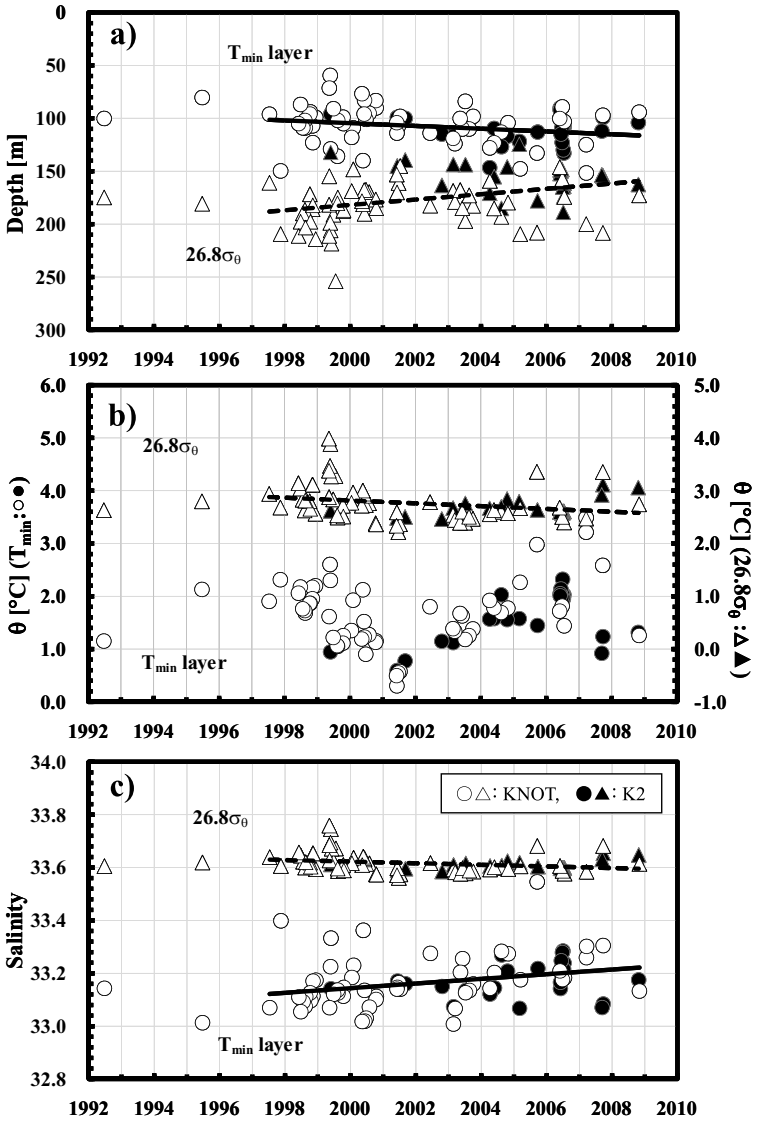

Fig. 4. Temporal variations of depth (a), θ (b) and salinity (c) from 1992 to 2008 in the temperature minimum ($T_{\min}$, circles) and $26.8\sigma_\theta$ (triangles) layers at stations KNOT (open symbols) and K2 (solid symbols); note the shifted scales for $T_{\min}$ (left) and $26.8\sigma_\theta$ (right) in panel (b). The depths in the $T_{\min}$ layer are those determined from continuous CTD data (1 db resolution). Where significant ($P < 0.05$), linear regressions for 1997 to 2008 are shown for the $T_{\min}$ (solid lines) and $26.8\sigma_\theta$ (dashed lines) layers.

Table 1. Rates of increase for DIC and related properties in the western subarctic gyre from 1997 to 2008

Layer	Depth (m)[a]	Depth (m yr^{-1})	θ (°C yr^{-1})	Salinity (yr^{-1})	AOU (μmol kg^{-1} yr^{-1})	TA (μmol kg^{-1} yr^{-1})	$\Delta C^* + C_{280}$ (μmol kg^{-1} yr^{-1})
$T_{\min.}$	108 ± 17	**1.3 ± 0.6**	0.039 ± 0.021	**0.009 ± 0.003**	**−2.1 ± 0.9**	**1.6 ± 0.2**	**1.3 ± 0.3**
$26.6\sigma_\theta$	121 ± 13	**−1.3 ± 0.4**	−0.020 ± 0.024	−0.002 ± 0.002	**−2.8 ± 0.8**	**0.9 ± 0.1**	**1.5 ± 0.3**
$26.7\sigma_\theta$	146 ± 16	**−2.0 ± 0.5**	−0.028 ± 0.016	−0.003 ± 0.002	**−3.0 ± 0.6**	**0.8 ± 0.1**	**1.4 ± 0.3**
$26.8\sigma_\theta$	175 ± 23	**−2.4 ± 0.8**	**−0.025 ± 0.011**	**−0.003 ± 0.001**	**−1.8 ± 0.5**	**0.5 ± 0.1**	**1.3 ± 0.2**
$26.9\sigma_\theta$	222 ± 32	−2.2 ± 1.2	0.012 ± 0.010	−0.001 ± 0.001	−0.4 ± 0.6	**0.5 ± 0.1**	**0.8 ± 0.2**
$27.0\sigma_\theta$	287 ± 37	−1.3 ± 1.4	−0.004 ± 0.007	0.000 ± 0.001	−0.3 ± 0.6	**0.5 ± 0.1**	**0.7 ± 0.2**
$27.1\sigma_\theta$	375 ± 38	−0.3 ± 1.4	−0.004 ± 0.007	0.000 ± 0.001	−0.2 ± 0.5	**0.5 ± 0.1**	0.4 ± 0.2

Note: Error values are the *SE* of the slope of the linear regression. Bold numbers indicate significant rates derived from linear regressions ($P < 0.05$).
[a]Averages and standard deviations at the isopycnal surfaces.

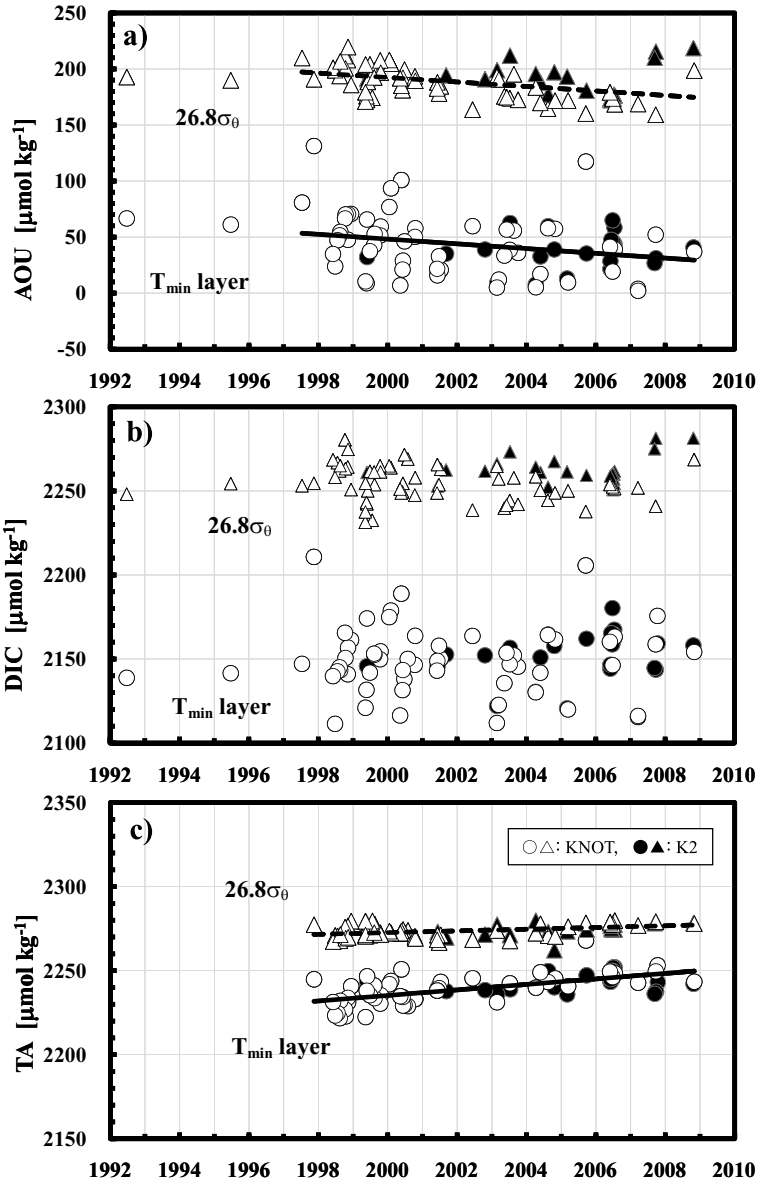

Fig. 5. Temporal variations of AOU (a), DIC (b) and TA (c) for 1992 to 2008 in the temperature minimum ($T_{\min}$, circles) and $26.8\sigma_\theta$ (triangles) layers at stations KNOT (open symbols) and K2 (solid symbols). Where significant ($P < 0.05$), linear regressions for 1997 to 2008 are shown for the $T_{\min}$ (solid lines) and $26.8\sigma_\theta$ (dashed lines) layers.

The change of DIC from the pre-industrial period caused by the oceanic uptake of CO_2 from the atmosphere through gas exchange (ΔC^*) is defined as follows:

$$\Delta C^* = \mathrm{DIC_m} - 117/170\mathrm{AOU_m} - 0.5(\mathrm{TA_m} - \mathrm{TA^\circ} + 16/170\mathrm{AOU_m}) + 106/104N^* - C_{\mathrm{eq280}},$$

where $\mathrm{DIC_m}$, $\mathrm{AOU_m}$ and $\mathrm{TA_m}$ are the measured values. $\mathrm{TA^\circ}$ is the preformed TA estimated using the equation of Sabine et al. (2002). The effect of decomposition from N^* would be small, but not trivial: Watanabe et al. (2008) demonstrated a linear increase of N^* on $26.8\sigma_\theta$ surface superimposed on a bidecadal oscillation. C_{eq280} is the theoretical DIC content of waters in equilibrium with the pre-industrial atmospheric CO_2 (280 μatm). Because C_{eq280} over time remains constant and its trend can be cancelled out, we calculated $\Delta C^* + C_{\mathrm{eq280}}$ and its trend represents the DIC increase caused by the uptake of CO_2 from the atmosphere through the gas exchange at the air–sea interface.

$\Delta C^* + C_{\mathrm{eq280}}$ has significantly increased at 0.7–1.5 (average 1.2 ± 0.3) μmol kg^{-1} yr^{-1} ($P < 0.05$) (Fig. 6, Table 1). These estimated increases in the winter mixed layer and upper intermediate water ($T_{\min}$ and $26.6\sigma_\theta$–$26.8\sigma_\theta$ layers), which are between 100 and 200 m thick, are greater than those in deeper water ($26.9\sigma_\theta$–$27.0\sigma_\theta$); $\Delta C^* + C_{\mathrm{eq280}}$ has remained unchanged below $27.1\sigma_\theta$. We estimated the increase of DIC accumulated in the water column to be 0.15 ± 0.04 mol m^{-2} yr^{-1} in the surface mixing layer and 0.25 ± 0.07 mol m^{-2} yr^{-1} in the intermediate

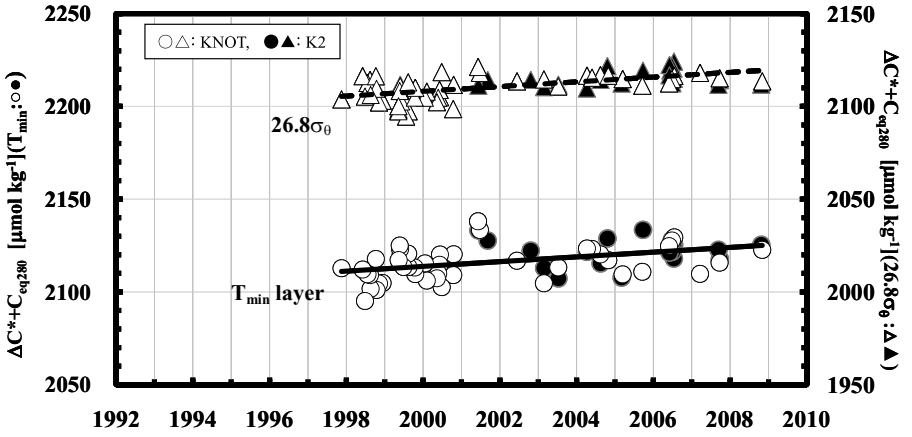

Fig. 6. Temporal variations of $\Delta C^* + C_{eq280}$ from 1992 to 2008 in the temperature minimum (T_{min}, circles) and 26.8σ_θ (triangles) layers at stations KNOT (open symbols) and K2 (solid symbols); note the shifted scales for T_{min} (left) and 26.8σ_θ (right). Where significant ($P < 0.05$), linear regressions for 1997 to 2008 are shown for the T_{min} (solid lines) and 26.8σ_θ (dashed lines) layers.

water (100–400 m), using the $\Delta C^* + C_{eq280}$ increase and the thickness of the average depth on each isopycnal surface from T_{min} to 27.1σ_θ at increments of 0.1σ_θ (Table 1). The total DIC inventory change in the surface and intermediate waters (0.40 ± 0.08 mol m^{-2} yr^{-1}; maximum depth ~400 m) is related to the CO_2 uptake rate; this value is similar to that previously reported in the subarctic western North Pacific [0.66 ± 0.22 mol m^{-2} yr^{-1}; maximum depth ~900 m; 1973–1993 (Ono et al., 2000)] and in the global ocean [0.51 ± 0.09 mol m^{-2} yr^{-1}; 1990s (Denman et al., 2007)].

This estimated inventory increase in the western subarctic gyre is higher than the anthropogenic CO_2 inventory increase in the Alaskan gyre (>45°N along 152°W) (<0.2 mol m^{-2} yr^{-1}; maximum depth < ~400 m; 1991/1992–2005/2006) estimated using an extended multiple linear regression technique (Sabine et al., 2008). This different value is the reason why the decadal DIC increase caused by the uptake of CO_2 from the atmosphere in the western subarctic gyre is larger than that in the Alaskan gyre despite the same penetration depth in the two gyres.

3.4. *Factors controlling the DIC increase due to air–sea CO_2 gas exchange*

The ΔC^* increase reflects the increase in anthropogenic CO_2 and the temporal variation in the CO_2 difference between atmosphere and ocean in the surface mixed layer at the time of water mass formation (e.g. Gruber et al., 1996; Sabine et al., 2002).

The $\Delta C^* + C_{eq280}$ increase in the T_{min} layer in the subarctic western North Pacific would be affected by not only the increase of anthropogenic CO_2 but also the temporal variation of a strong CO_2 source during winter, because the T_{min} layer is a remnant of the preceding winter mixed layer (e.g. Osafune and Yasuda, 2006). The western subarctic areas along the Kuril and western Aleutian arcs are strong CO_2 sources during winter owing to convective mixing of deep waters rich in respired CO_2 (e.g. Takahashi et al., 2006). This seasonal variation of pCO_2 has an opposite pattern to that of other open ocean time-series sites (ALOHA, BATS and OSP) (e.g. Tsurushima et al., 2002), because the primary causes of seasonal change in pCO_2 in the subarctic region (K2 and KNOT) and these other time-series sites are seasonal changes in DIC and temperature, respectively (e.g. Takahashi et al., 2006). The temporal variation of CO_2 emission in winter must affect that of DIC in the T_{min} layer. If the winter increase rate of atmospheric CO_2 were higher than that of oceanic CO_2 from year-to-year, then the oceanic CO_2 uptake over time in this region would increase as a result of the reduction of CO_2 emission in winter due to decrease in the CO_2 difference between atmosphere and ocean.

The decadal increases of $\Delta C^* + C_{eq280}$ we observed in the T_{min} layer (1.3 ± 0.3 μmol kg^{-1} yr^{-1}) were higher than expected from oceanic equilibration with increased anthropogenic CO_2 in the atmosphere (0.7 μmol kg^{-1} yr^{-1}), when calculated using the increase of atmospheric CO_2 (1.9 ppm yr^{-1}) (Foster et al., 2007) and the Revelle factor in the T_{min} layer (15.6 ± 0.4) at constant TA. This Revelle factor is consistent with previous results in winter (Takahashi et al., 2006). This $\Delta C^* + C_{eq280}$ increase was larger than the anthropogenic DIC increase since the 1990s at other open North Pacific stations [<1.1 μmol kg^{-1} yr^{-1}; <30°N along 149°E (WHP P10) (Murata et al., 2009), <1.0 μmol kg^{-1} yr^{-1}; 145°E–140°W along 30°N (WHP P02), 0–55°N along 152°W (WHP P16) (Sabine et al., 2008)], and is comparable to higher anthropogenic CO_2 increases associated with the Kuroshio and California Currents on both edges of the basin (<1.5 μmol kg^{-1} yr^{-1}; WHP P02) (Sabine et al., 2008).

The CO_2 emission in winter is estimated from the difference between atmospheric and oceanic xCO_2. We calculated oceanic xCO_2 by using the values of DIC and TA in the mixing layer (early April) (DIC_{win}, TA_{win}). Phosphate and nitrate in the winter mixing layer also were calculated (PO_{4win}, NO_{3win}). DIC, TA,

phosphate and nitrate in the T_{min} layer ($DIC_{T_{min}}$, $TA_{T_{min}}$, $PO_{4T_{min}}$, $NO_{3T_{min}}$) are referred to as DIC_{win}, TA_{win}, PO_{4win} and NO_{3win}. Salinity normalized values of DIC, TA, phosphate and nitrate ($nDIC_{win}$, nTA_{win}, nPO_{4win} and nNO_{3win}) were used to remove the influence of local evaporation and precipitation change, because salinity in the T_{min} layer increased from 1997 to 2008 (Fig. 4c). A salinity of 33.1 was chosen as the constant to correct DIC, TA and nutrient data, as this represents the mean salinity observed in the T_{min} layer over this period. For example, $nDIC_{win}$ was calculated by the following equation:

$$nDIC_{win} = DIC_{win} \times 33.1/Sal_{win},$$

where Sal_{win} is salinity in the T_{min} layer. The values of DIC, AOU, PO_4 and NO_3 in the T_{min} layer ($DIC_{T_{min}}$,$AOU_{T_{min}}$, $PO_{4T_{min}}$and $NO_{3T_{min}}$) were annual minima in winter (Figs 3e, f and h), whereas $TA_{T_{min}}$ had no a distinct seasonal variation (Fig. 3g). This increase of observed $DIC_{T_{min}}$, $PO_{4T_{min}}$ and $NO_{3T_{min}}$ are caused by the decomposition of organic matter after the previous winter (Figs 3e, f and h). We assumed that DO in the winter mixed layer is homogeneously saturated (i.e. AOU = 0) (e.g. Tsurushima et al., 2002), because the degree of saturation of DO in early April is ∼100% (98 ± 2%) because of the strong vertical mixing and air–sea exchange. DIC_{win}, PO_{4win} and NO_{3win} were obtained from the observed $DIC_{T_{min}}$, $PO_{4T_{min}}$ and $NO_{3T_{min}}$ and decomposition with the following equations:

$$DIC_{win} = DIC_{T_{min}} - C/-O_2(=117/170) \times AOU_{T_{min}},$$

$$PO_{4win} = PO_{4T_{min}} - P/-O_2(=1/170) \times AOU_{T_{min}},$$

$$NO_{3win} = NO_{3T_{min}} - N/-O_2(=16/170) \times AOU_{T_{min}},$$

where C/–O_2, P/–O_2 and N/–O_2 are the stoichiometric ratios of carbon, phosphorus and nitrogen to oxygen during the decomposition of organic matter (Anderson and Sarmiento, 1994). We estimated the xCO_2 of surface seawater in winter from $nDIC_{win}$ and nTA_{win} (Figs 7a and b). The contents of atmospheric xCO_2 in late winter (at the beginning of April) are cited by GLOBALVIEW-CO2 (2009) from 1997 to 2008 at 44.4°N.

The slope of the linear regression of oceanic xCO_2 on time was 0.7 ± 0.5 ppm yr^{-1} ($n = 68$), which was significant at the 90% confidence level ($P \leq 0.1$) (Fig. 7c). This linear regression model was fitted using the weighted least squares approach, because calculated xCO_2 in the ocean was dispersing from year-to-year. This annual dispersion was not significantly uniform by Kruskal–Wallis test ($P < 0.001$), which indicates the necessity of weights. We used the weights as the inverse of variance of oceanic xCO_2 every year and obtained the linear regression of oceanic xCO_2 in winter. This oceanic CO_2 increase is consistent with the direct measurement values from 1995 to 2008 near KNOT and K2 of 1.2–1.5 ppm yr^{-1} for oceanic pCO_2, within standard errors (Dr. Nakaoka, NIES, personal communication).

The increase of atmospheric xCO_2 (2.1 ± 0.0 ppm yr^{-1}, $n = 12$) in winter is significantly higher than that of oceanic xCO_2 by the comparison of the two linear regressions ($F < 0.001$) (Fig. 7c). This significance was tested by using the F-distribution of the maximum likelihood estimate of variance, because the regression of oceanic xCO_2 was fitted using the weighted least squares approach. The difference of xCO_2 between atmosphere and ocean was calculated to be 1.4 ± 0.5 ppm yr^{-1}. These results suggest that the declining CO_2 emissions in winter were due to the declining xCO_2 gradient between atmosphere and ocean over time.

The temporal change in the CO_2 source in winter could be caused by increase of TA in the winter mixed layer. In the CO_{2s} system calculation from the DIC change at constant TA in the seawater, the oceanic xCO_2 increase in the seawater is proportional to the DIC increase. If TA in the seawater increases over time, the oceanic xCO_2-increasing trend is smaller than that calculated by the increase of DIC under constant temperature and TA conditions. Applying this theoretical case to KNOT and K2, we estimated the oceanic xCO_2 increase to be 0.8 ppm yr^{-1} by using the increasing values computed from the regression lines of $nDIC_{win}$ (Fig. 7a, DIC = 1.2 × year − 368.4) and nTA_{win} (Fig. 7b, TA = 1.1 × year − 46.6) at constant T_{min} (1.63 °C, mean from 1997 to 2008) (Fig. 8). This estimated increase is similar to that by observed $nDIC_{win}$ and nTA_{win} (0.7 ± 0.5 ppm yr^{-1}, Fig. 7c) and is considerably smaller than that using computed $nDIC_{win}$ increasing values and a constant nTA_{win} value (2230 μmol kg^{-1} in 1997; 3.9 ppm yr^{-1}) (Fig. 8). Thus, the increasing trend of nTA_{win} could inhibit the decadal increase of oceanic xCO_2 against the $nDIC_{win}$ increase, which suggests a reduction of CO_2 emissions in winter. This indicates that TA increase favours the uptake of CO_2 in the ocean.

If increases of atmospheric and oceanic xCO_2 in winter continue in the future at the same rates as those from 1997 to 2008, the gradient between the atmosphere and ocean in winter might gradually decrease with time. Additional time-series data are required to confirm the factors controlling the temporal change of CO_2 emission in winter and to evaluate this speculation.

In addition to decadal increase of $nDIC_{win}$ and nTA_{win}, the salinity, depth, nPO_{4win} and nNO_{3win} in the winter mixed layer (T_{min} layer) also have significantly increased during the years 1997–2008 ($P < 0.05$) (Figs 4a and c and 7d and e), while σ_θ remained constant (Fig. 7f). The increasing trend of nTA_{win}, nPO_{4win} and nNO_{3win} may be caused by the enhanced winter convective mixing of deep waters rich in DIC, TA and nutrients. This increasing of nPO_{4win} (Fig. 7d) will follow the increasing trend of phosphate during the 1989–1993 period in the winter mixed layer of the subarctic western North Pacific (Ono et al., 2002). In contrast, multi-decadal decreasing trends of salinity, density and phosphate in the winter mixed layer from the 1970s to the 1990s in the Oyashio region and near the subarctic western North Pacific were thought to have been caused by the

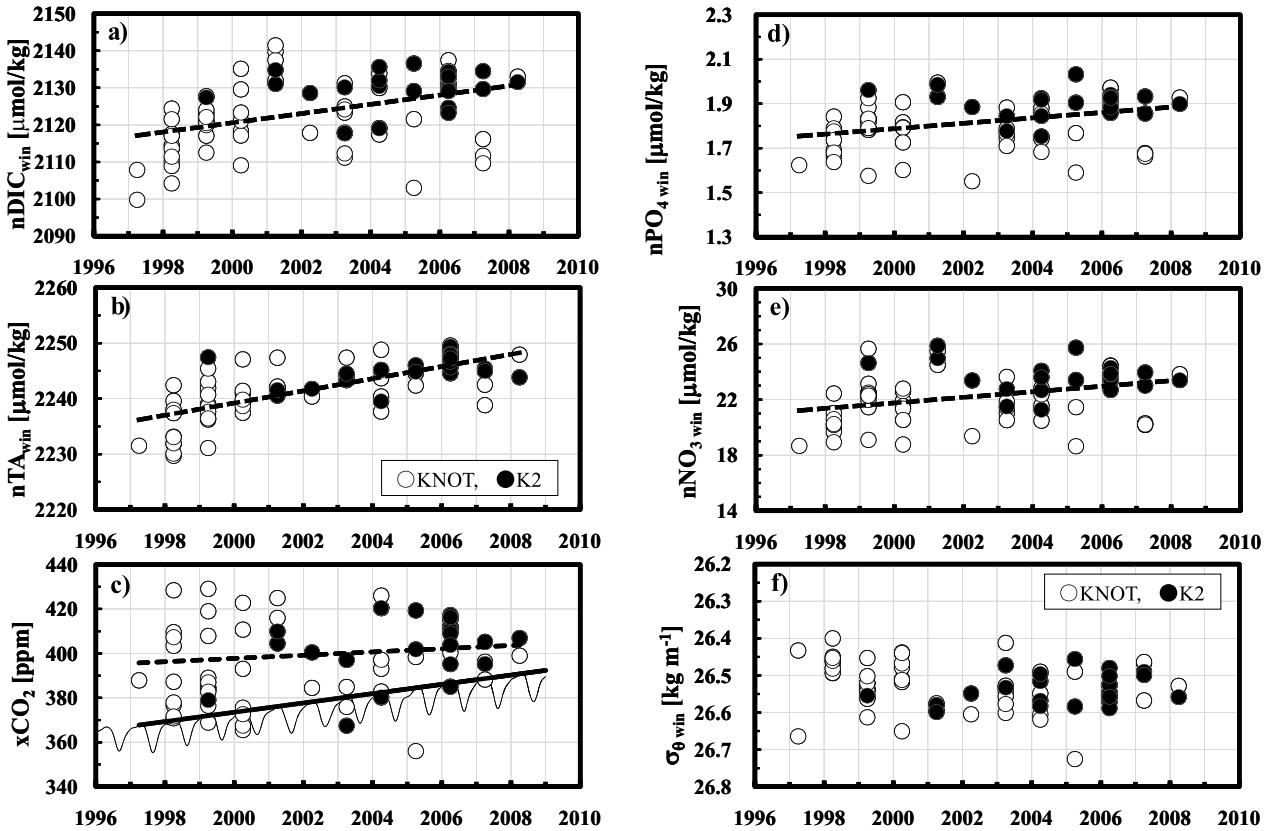

Fig. 7. Temporal variations of (a) DIC (nDIC$_{win}$), (b) TA (nTA$_{min}$), (c) xCO$_2$, mixing ratio of CO$_2$ by volume in the dried air, in the atmosphere (thin curve) at 44.4°N (GLOBAL VIEW-CO$_2$, 2009) and in the ocean (circles), (d) phosphate (nPO$_{4win}$), (e) nitrate (nNO$_{3win}$) and (f) potential density ($\sigma_{\theta win}$) at stations KNOT (open symbols) and K2 (solid symbols) in the winter mixed layer [temperature minimum (T_{min}) layer]. Temperature minimum is defined as the remnant of the winter mixed layer in early April. Salinity-normalized DIC (nDIC$_{win}$), TA (nTA$_{win}$), phosphate (nPO$_{4win}$) and nitrate (nNO$_{3win}$) data were used to remove the influence of local evaporation and precipitation. Values of oceanic xCO$_2$ in the winter mixed layer were calculated between nTA$_{win}$ and nDIC$_{win}$. Regression lines for 1997 to 2008 are shown for nDIC$_{win}$ (dotted line, 1.4 ± 0.3 μmol kg^{-1} yr^{-1}, $P < 0.0001$); nTA$_{win}$ (dotted line, 1.1 ± 0.1 μmol kg^{-1} yr^{-1}, $P < 0.05$); atmospheric xCO$_2$ in winter (solid line; 2.1 ± 0.0 ppm yr^{-1}, $P < 0.001$); oceanic xCO$_2$ in winter (dashed line; 0.7 ± 0.5 ppm yr^{-1}, $P \leq 0.10$); nPO$_{4win}$ (dotted line, 0.012 ± 0.004 μmol kg^{-1} yr^{-1}, $P < 0.05$); and nNO$_{4win}$ (dotted line, 0.20 ± 0.06 μmol kg^{-1} yr^{-1}, $P < 0.05$).

occurrence of surface stratification (Ono et al., 2001, 2002). Moreover, the temporal variability of depth and CO$_2$ emissions from the winter mixed layer must be relevant to atmospheric forcing (wind speed, etc.). The temporal variations of AOU on the isopycnal surface 26.7–27.2σ_θ in the Oyashio region and wintertime wind stress curl anomaly around this region are negatively and positively correlated with the bidecadal component of NPI, respectively (Ono et al., 2001; Ishi and Hanawa, 2005). Because DIC is positively correlated with AOU in the subsurface water ($r = 0.99$) due to the decomposition of organic matter, temporal variation of DIC also possibly has a bidecadal oscillation. Further investigation of the atmospheric effect is required to detect whether there is enhanced winter convective mixing of deep waters or not. The relationships among temporal variability of winter CO$_2$ emissions and atmospheric forcing or climate index must be investigated in the near future. In the future, more accurate and longer time-series data will be required to evaluate these speculations.

4. Summary

DIC and related chemical species have been measured from 1992 to 2008 at Stations KNOT (44°N, 155°E) and K2 (47°N, 160°E) in the subarctic western North Pacific in the western subarctic gyre. The surface mixed layer there in winter is a source of atmospheric CO$_2$ owing to strong vertical mixing (~100 m) and from spring to fall it is a sink for CO$_2$ because of biological production (e.g. Tsurushima et al., 2002) (Fig. 3i). This seasonal variation of pCO$_2$ has an opposite pattern to that of other time-series sites (ALOHA, BATS and OSP) (e.g. Tsurushima et al., 2002), because the primary cause for seasonal change in the subarctic region is seasonal DIC change (e.g. Takahashi et al.,

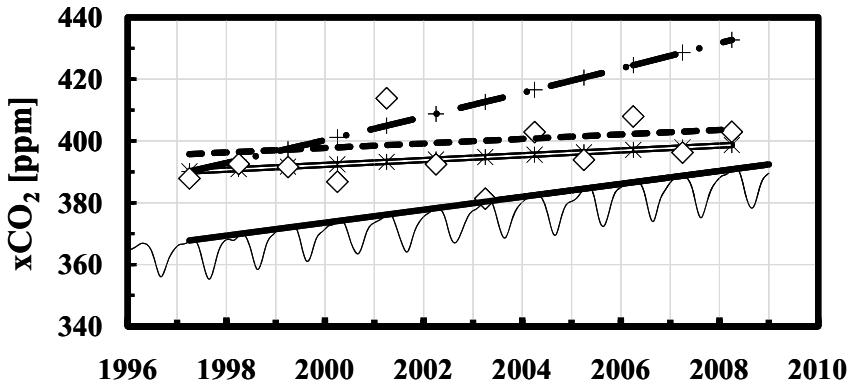

Fig. 8. Temporal variations of atmospheric CO_2 (thin line) at 44.4°N [GLOBAL VIEW-CO2, 2009]; means of oceanic xCO_2 for the subarctic western North Pacific (diamonds); theoretical xCO_2 in the ocean calculated using increasing values computed between the regression lines of $n\mathrm{DIC}_{\mathrm{win}}$ ($n\mathrm{DIC}_{\mathrm{win}} = 1.2 \times \mathrm{year} - 368.4$, Fig. 7a) and $n\mathrm{TA}_{\mathrm{win}}$ (TA $= 1.1 \times$ year $- 46.6$, Fig. 7b) at constant temperature minimum (T_{min}) (1.63 °C, mean from 1997 to 2008) (asterisks); and that using computed $n\mathrm{DIC}_{\mathrm{win}}$ increasing values and constant value of $n\mathrm{TA}_{\mathrm{win}}$ (2230 μmol kg^{-1} in 1997, Fig. 7b) (pluses) and T_{min} from 1997 to 2008 at stations KNOT and K2 in the winter mixed layer. Regression lines for 1997 to 2008 are shown for atmospheric CO_2 in winter (solid line; 2.1 ± 0.0 ppm yr^{-1}, $P < 0.001$); oceanic CO_2 in winter calculated between observed $n\mathrm{DIC}_{\mathrm{win}}$ and $n\mathrm{TA}_{\mathrm{win}}$ (dashed line; 0.7 ± 0.5 ppm yr^{-1}, $P \leq 0.10$); theoretical CO_2 in the ocean calculated using increasing values of $n\mathrm{DIC}_{\mathrm{win}}$ and $n\mathrm{TA}_{\mathrm{win}}$ at constant T_{min} (doublet line, 0.8 ppm yr^{-1}); and that calculated using the increasing values of $n\mathrm{DIC}_{\mathrm{win}}$ and constant value of $n\mathrm{TA}_{\mathrm{win}}$ and T_{min} (chain line, 3.9 ppm yr^{-1}).

2006). The temporal change of CO_2 emission in winter must affect that of DIC in the T_{min} layer. Decadal DIC increase below the T_{min} layer is affected not only by the increase of anthropogenic CO_2 but also by temporal change of a strong CO_2 source during winter, because the typical water column structure here has the T_{min} layer at ∼26.5σ_θ (∼100 m) (Figs 2 and 3d), which is the remnant of the mixed layer from the preceding winter.

To estimate the decadal increase of DIC resulting from the uptake of CO_2 from gas exchange with the atmosphere, we corrected DIC for the contribution of the biological activity by calculating ΔC^* (e.g. Gruber et al., 1996; Sabine et al., 2002). Decadal changes of corrected DIC have significantly increased at 0.7–1.5 (avg. 1.2 ± 0.2) μmol kg^{-1} yr^{-1} in the subsurface water from 1997 to 2008 (Fig. 6, Table 1). These estimated increases in the winter mixed layer and upper intermediate water (T_{min} layer and 26.6–26.8σ_θ; 100–200 m) are higher than those in the next deeper water layer (26.9–27.0σ_θ; 200–300 m) and have remained unchanged below 27.1σ_θ (∼400 m). We estimated the water column inventory of CO_2 increase to be 0.40 ± 0.08 mol m^{-2} yr^{-1}, which is similar to those previously reported for the same region (Ono et al., 2000) and for the global ocean (Bindoff et al., 2007).

The decadal DIC increase by the uptake of CO_2 from the atmosphere into the winter mixed layer (T_{min} layer) would be affected not only by the increase of anthropogenic CO_2 but also the reduction of CO_2 emission in winter. The estimated DIC increase in the T_{min} layer and in the 26.6–26.8σ_θ layer (1.3–1.5 μmol kg^{-1} yr^{-1}) was higher than that expected from oceanic equilibration with increased anthropogenic CO_2 in the atmosphere (0.7 μmol kg^{-1} yr^{-1}) and anthropogenic DIC increase since the 1990s in the other open North Pacific stations (<1.1 μmol kg^{-1} yr^{-1}) (Sabine et al., 2008; Murata et al., 2009). The increase of atmospheric xCO_2 (2.1 ± 0.0 ppm yr^{-1}) in winter (early April) is markedly higher than that of oceanic xCO_2 in winter calculated from observed $\mathrm{DIC}_{T_{\mathrm{min}}}$ and $\mathrm{TA}_{T_{\mathrm{min}}}$ (0.7 ± 0.5 ppm yr^{-1}) (Fig. 7c), which suggests that the reduction of CO_2 emission in winter is due to a decreasing xCO_2 gradient between the atmosphere and ocean.

This temporal change of the CO_2 source in winter is possibly caused by an increase of $n\mathrm{TA}_{\mathrm{win}}$ in the winter mixed layer. The oceanic xCO_2 increase calculated from observed $\mathrm{DIC}_{T_{\mathrm{min}}}$ and $\mathrm{TA}_{T_{\mathrm{min}}}$ was considerably smaller than that calculated using computed $n\mathrm{DIC}_{\mathrm{min}}$ increasing values and constant T_{min} (1.63 °C, mean from 1997 to 2008) and $n\mathrm{TA}_{\mathrm{win}}$ (2230 μmol kg^{-1}in 1997; 3.9 ppm yr^{-1}) (Fig. 8). Thus, the increasing trend of $n\mathrm{TA}_{\mathrm{win}}$ would inhibit decadal increase of oceanic xCO_2 against $n\mathrm{DIC}_{\mathrm{win}}$ increasing, which suggests the reduction of CO_2 emission in winter. This indicates that TA increase favours the uptake of CO_2 in the ocean. Additional time-series data are required to confirm the factors controlling the temporal change of CO_2 emission in winter. Moreover, because CO_2 efflux from the winter mixed layer must be relevant to atmospheric forcing, the relationships between temporal variability of winter CO_2 emissions and atmospheric forcing must be investigated in the near future.

5. Acknowledgments

We acknowledge the staff of Mutsu Institute for Oceanography, JAMSTEC and the captains and crews of the R/V *Mirai*, R/V *Natsushima*, T/S *Hokusei Maru*, T/S *Oshoro Maru*, R/V *Bosei Maru*, R/V *Hakurei* No. 2, R/V *Kaiyo* and R/V *Hakuho Maru* for their kind cooperation in the collection of samples and

hydrographic measurements during the 1992–2008 cruises. We thank Drs. Y. Kumamoto, H. Kawakami, K. Sasaki, Y. Nakano and T. Fujiki and Mr. K. Matsumoto of JAMSTEC; Dr. S. Nakaoka of the National Institute for Environmental Studies; Drs. T. Midorikawa and M. Ishii of the Meteorological Research Institute; Dr. T. Tanaka of the Japan Atomic Energy Agency; Dr. T. Ono of the Fisheries Research Agency; and Drs. Y. W. Watanabe, H. Y. Inoue and S. Tsunogai of Hokkaido University for their valuable comments and discussion; Dr. H. Narita of Tokai University and Dr. K. Imai of Hokkaido University for their great support onboard; and the staff of Marine Works Japan Co., Ltd. who worked as marine technicians onboard. Finally, we also express our deep thanks to three anonymous reviewers who gave us many useful comments.

References

Anderson, L. A. and Sarmiento, J. L. 1994. Redfield ratios of remineralization determined by nutrient data analysis. *Global Biogeochem. Cycles* **8**, 65–80.

Bates, N. R., Pequignet, A. C., Johnson, R. J. and Gruber, N. 2002. A short-term sink for atmospheric CO_2 in Subtropical Mode Water of the North Atlantic Ocean. *Nature* **420**, 489–493.

Bindoff, N. L., Willebrand, J., Artale, V., Cazenave, A., Gregory, J. and co-authors. 2007. Observations: oceanic climate change and sea level In: *Climate Change 2007: The Physical Science Basis—Contribution of Working Group I to the Fourth Assessment Report of the Intergovernmental Panel on Climate Change*. (eds S. Solomon and co-editors). Cambridge University Press, New York, 385–432.

de Boyer Montégut, C., Madec, G., Fischer, A. S., Lazar, A. and Iudicone, D. 2004. Mixed layer depth over the global ocean: an examination of profile data and a profile-based climatology. *J. Geophys. Res.* **109**, C12003, doi:10.1029/2004JC002378.

Deutsch, C., Gruber, N., Key, R. M., Sarmiento, J. L. and Ganachaud, A. 2001. Denitrification and N2 fixation in the Pacific Ocean. *Global Biogeochem. Cycles* **15**, 483–506.

Denman, K. L., Brasseur, G., Chidthaisong, A., Ciais, P., Cox, P. M. and co-authors. 2007. Couplings between changes in the climate system and biogeochemistry. In: *Climate Change 2007: The Physical Science Basis—Contribution of Working Group I to the Fourth Assessment Report of the Intergovernmental Panel on Climate Change* (eds S. Solomon and co-editors). Cambridge University Press, New York, 499–588.

Dickson, A. G. and Millero, F. J. 1987. A comparison of the equilibrium constants for the dissociation of carbonic acid in seawater media. *Deep Sea Res. Part I* **34**, 1733–1743.

Dore, J. E., Lukas, R., Sadler, D. W. and Karl, D. M. 2003. Climate-driven changes to the atmospheric CO_2 sink in the subtropical North Pacific Ocean. *Nature* **424**, 754–757.

Feely, R. A., Sabine, C. L., Lee, K., Millero, F. J., Lamb, M. F. and co-authors. 2002. In situ calcium carbonate dissolution in the Pacific Ocean. *Global Biogeochem. Cycles* **16**, GB1144, doi:10.1029/2002GB001866.

Foster, P., Ramaswamy, V., Artaxo, P., Berntsen, T., Betts, R., and co-authors. 2007. Changes in Atmospheric Constituents and in Radiative Forcing. In: *Climate Change 2007: The Physical Science Basis—Contribution of Working Group I to the Fourth Assessment Report of the Intergovernmental Panel on Climate Change* (eds S. Solomon and co-editors). Cambridge University Press, New York, 129–234.

Gruber, N., Sarmiento, J. L. and Stocker, T. F. 1996. An improved method for detecting anthropogenic CO_2 in the oceans. *Global Biogeochem. Cycles* **10**, 809–837.

GLOBALVIEW-CO_2. 2009. Cooperative Atmospheric Data Integration Project–Carbon Dioxide. CD-ROM, NOAA ESRL, Boulder, Colorado.

Honda, M. C., Kawakami, H., Sasaoka, K., Watanabe, S. and Dickey, T. 2006. Quick transport of primary produced organic carbon to the ocean interior. *Geophys. Res. Lett.* **33**, L16603, doi:10.1029/2006GL026466.

Ishi, Y. and Hanawa, K. 2005. Large-scale variabilities of wintertime wind stress curl field in the North Pacific and their relation to atmosphere teleconnection patterns. *Geophys. Res. Lett.* **32**, L10607, doi:10.1029/2004GL022330.

Johnson, G. C., Rudnick, D. L. and Taft, B. A. 1994. Bottom water variability in the Samoa Passage. *J. Mar. Res.* **52**, 177–196.

Kawakami, H., Honda, M. C., Wakita, M. and Watanabe, S. 2007. Time-series observation of dissolved inorganic carbon and nutrients in the northwestern North Pacific. *J. Oceanogr.* **63**, 967–982.

Mecking, S., Langdon, C., Feely, R. A., Sabine, C. L., Deutsch, C. A., and co-authors. 2008. Climate variability in the North Pacific thermocline diagnosed from oxygen measurements: an update based on the U.S. CLIVAR/CO_2 Repeat Hydrography cruises. *Global Biogeochem. Cycles* **22**, GB3015, doi:10.1029/2007GB003101.

Mehrbach, C., Culberson, C. H., Hawley, J. E. and Pytkowicz, R. M. 1973. Measurement of the apparent dissociation constants for carbonic acid in seawater at atmospheric pressure. *Limnol. Oceanogr.* **18**, 897–907.

Murata, A., Kumamoto, Y., Sasaki, K., Watanabe, S. and Fukasawa, M. 2009. Decadal increases of anthropogenic CO_2 along 149°E in the western North Pacific. *J. Geophys. Res.* **114**, C04018, doi:10.1029/2008JC004920.

Ono, T., Watanabe, Y. W. and Watanabe, S. 2000. Recent increase of DIC in the western North Pacific. *Mar. Chem.* **72**, 317–328.

Ono, T., Midorikawa, T., Watanabe, Y. W., Tadokoro, K. and Saino, T. 2001. Temporal increases of phosphate and apparent oxygen utilization in the subsurface waters of western subarctic Pacific from 1968 to 1998. *Geophys. Res. Lett.* **28**, 3285–3288.

Ono, T., Tadokoro, K., Midorikawa, T., Nishioka, J. and Saino, T. 2002. Multi-decadal decreases of net community production in the western subarctic North Pacific. *Geophys. Res. Lett.* **29**, doi:10.1029/2001GL014332.

Osafune, S. and Yasuda, I. 2006. Bidecadal variability in the intermediate waters of the northwestern subarctic Pacific and the Okhotsk Sea in relation to 18.6-year period nodal tidal cycle. *J. Geophys. Res.* **111**, C05007, doi:10.1029/2005JC003277.

Pierrot, D., Lewis, E. and Wallace, D. W. R. 2006. MS Excel program developed for CO_2 system calculations. *ORNL/CDIAC-105*. U.S. Dep. of Energy, Oak Ridge, Tennessee.

Sabine, C. L., Feely, R. A., Key, R. M., Bullister, J. L., Millero, F. J. and co-authors. 2002. Distribution of anthropogenic CO_2 in the Pacific Ocean. *Global Biogeochem. Cycles* **16**(4), 1083, doi:10.1029/2001GB001639.

Sabine, C. L., Feely, R. A., Millero, F. J., Dickson, A. G., Langdon, C. and co-authors. 2008. Decadal changes in Pacific carbon. *J. Geophys. Res.* **113**, C07021, doi:10.1029/2007JC004577.

Santana-Casiano, J. M., González-Dávila, M., Rueda, M.-J., Llinás, O. and González-Dávila, E.-F. 2007. The interannual variability of oceanic CO_2 parameters in the northeast Atlantic subtropical gyre at the ESTOC site. *Global Biogeochem. Cycles* **21**, GB1015, doi:10.1029/2006GB002788.

Sarma, V. V. S. S., Ono, T. and Saino, T. 2002. Increase of total alkalinity due to shoaling of aragonite saturation horizon in the Pacific and Indian Oceans: influence of anthropogenic carbon inputs. *Geophys. Res. Lett.* **29**(20), 1971, doi:10.1029/2002GL015135.

Stuiver, M., Quay, P. D. and Ostlund, H. G. 1983. Abyssal water carbon-14 distribution and the age of the world oceans. *Science* **219**, 849–851.

Takahashi, T., Sutherland, S. C., Feely, R. A. and Wanninkhof, R. 2006. Decadal change of the surface water pCO_2 in the North Pacific: a synthesis of 35 years of observations. *J. Geophys. Res.* **111**, C07S05, doi:10.1029/2005JC003074.

Takahashi, T., Sutherland, S. C., Wanninkhof, R., Sweeney, C., Feely, R. A. and co-authors. 2009. Climatological mean and decadal change in surface ocean pCO_2, and net sea–air CO_2 flux over the global oceans. *Deep Sea Res. Part II* **56**, 554–577.

Tanaka, T., Watanabe, Y. W., Watanabe, S. and Noriki, S. 2003. Oceanic Suess effect of $\delta^{13}C$ in subpolar region: the North Pacific. *Geophys. Res. Lett.* **30**(22), 2159, doi:10.1029/2003GL018503.

Tsurushima, N., Nojiri, Y., Imai, K. and Watanabe, S. 2002. Seasonal variations of carbon dioxide system and nutrients in the surface mixed layer at Station KNOT (44°N, 155°E) in the subarctic North Pacific. *Deep Sea Res. Part II* **49**, 5377–5394.

Trenberth, K. E. and Hurrell, J. W. 1994. Decadal atmosphere-ocean variations in the Pacific. *Clim. Dyn.* **9**, 303–319.

Yasuda, I., Okuda, K. and Shimizu, Y. 1996. Distribution and modification of the North Pacific Intermediate Water in the Kuroshio-Oyashio Interfrontal zone. *J. Phys. Oceanogr.* **26**, 448–465.

Wakita, M., Watanabe, S., Watanabe, Y. W., Ono, T., Tsurushima, N. and co-authors. 2005. Temporal change of dissolved inorganic carbon in the subsurface water at station KNOT (44°N, 155°E) in the western North Pacific subpolar region. *J. Oceanogr.* **61**, 129–139.

Watanabe, Y. W., Ono, T., Shimamoto, A., Sugimoto, T., Wakita, M. and co-authors. 2001. Probability of a reduction in the formation rate of the subsurface water in the North Pacific during the 1980s and 1990s. *Geophys. Res. Lett.* **28**(17), 3289–3292,

Watanabe, S., Honda, M. C., Murata, A. and Wakita, M. 2007. Hydrographic Data at Station K2 between 2001 and 2006. Japan Agency for Marine-Earth Science and Technology, Yokosuka, Japan. Available from: dmo@jamstec.go.jp.

Watanabe, Y. W., Shigemitsu, M. and Tadokoro, T. 2008. Evidence of a change in oceanic fixed nitrogen with decadal climate change in the North Pacific subpolar region. *Geophys. Res. Lett.* **35**, L01602, doi:10.1029/2007GL032188.

Weiss, R. F. 1970. The solubility of nitrogen, oxygen and argon in water and seawater. *Deep Sea Res.* **17**, 721–735.

Wong, C. S. and Chan, Y.-H. 1991. Temporal variations in the partial pressure and flux of CO_2 at ocean station P in the subarctic northeast Pacific Ocean. *Tellus* **43B**, 206–223.